LASER INTERFEROMETER GRAVITATIONAL WAVE OBSERVATORY
- LIGO -
CALIFORNIA INSTITUTE OF TECHNOLOGY
MASSACHUSETTS INSTITUTE OF TECHNOLOGY

Technical Note **LIGO-T2600323-v1** 09/25/2026

Data acquisition, signal processing, and noise characterization for the GQuEST experiment

Ciara Treanor
Boston College

California Institute of Technology
LIGO Project, MS 18-34
Pasadena, CA 91125
Phone (626) 395-2129
Fax (626) 304-9834
E-mail: info@ligo.caltech.edu

Massachusetts Institute of Technology
LIGO Project, Room NW17-161
Cambridge, MA 02139
Phone (617) 253-4824
Fax (617) 253-7014
E-mail: info@ligo.mit.edu

LIGO Hanford Observatory
Route 10, Mile Marker 2
Richland, WA 99352
Phone (509) 372-8106
Fax (509) 372-8137
E-mail: info@ligo.caltech.edu

LIGO Livingston Observatory
19100 LIGO Lane
Livingston, LA 70754
Phone (225) 686-3100
Fax (225) 686-7189
E-mail: info@ligo.caltech.edu

http://www.ligo.caltech.edu/

Contents

1 Introduction **2**

1.1 GQuEST 2

1.2 Cross-Correlation 3

2 Objectives **4**

3 Approach **4**

3.1 Photodiode Modifications 4

3.2 Photodiode Characterization 6

3.3 Data Acquisition System 8

3.4 Theoretical ADC Noise Floor and Required Runtime 12

3.5 17 MHz Laser Noise Measurement 14

4 Results **15**

5 Conclusion **17**

6 Acknowledgements **18**

1 Introduction

1.1 GQuEST

Theoretically, the quantum nature of gravity is expected to stochastically produce "geontropic" space-time fluctuations, or geometric fluctuations in space-time due to entropy [1]. The gravity from the quantum entanglement of space-time (GQuEST) experiment aims to detect these space-time fluctuations as evidence of quantum gravity as predicted by this theory. GQuEST will use a Michelson interferometer with 7 m long arms and a 1550 nm frequency-stabilized laser with a superconducting nanowire single-photon detector (SNSPD).

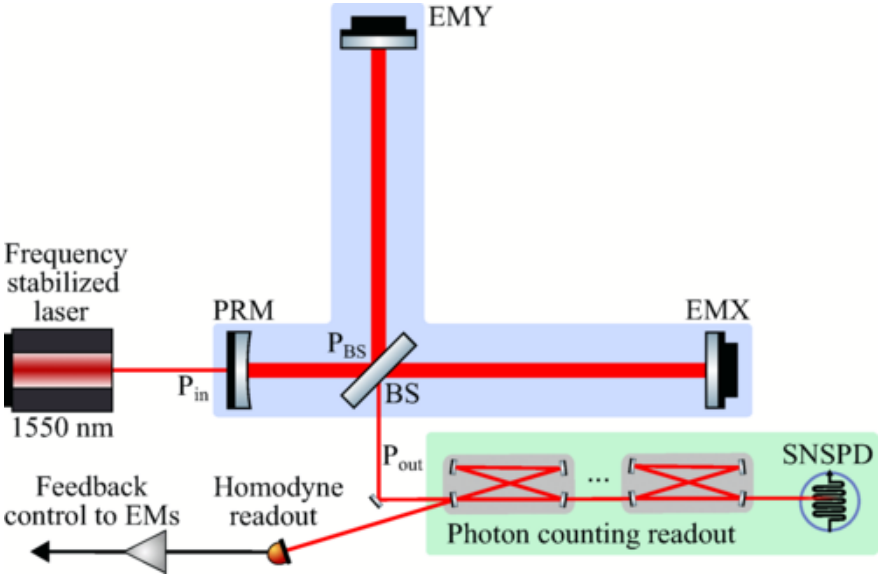


Figure 1: Simplified GQuEST experimental design [2].

The SNSPD will be used in addition to homodyne measurements to get a more precise readout not subject to the limit from photon shot noise. In homodyne, the system measures the signal times the local oscillator and retains phase information, an important metric for LIGO when measuring gravitational waves. Photon-counting filters out the local oscillator and removes phase information. GQuEST will be measuring what is believed to be the stochastic and broadband signal of spacetime fluctuations, meaning phase measurements are no longer necessary. Instead GQuEST will measure an optical power at the IFO output which corresponds to spacetime fluctuation amplitude. These fluctuations are theorized to occur at a specified frequency (roughly 17 MHz) where the experimental and background noise is at a minimum [2].

By measuring the cross-correlation between two independent interferometers, we can remove shot noise and examine any classical noise sources and systematic errors. The introduction of SNSPDs is a critical advancement; we will coherently combine light from two interferometers and use an individual photon-counting readout. This way, the experiment can extract Fisher

information regarding the path-length fluctuations much more efficiently than traditional homodyne systems, effectively bypassing the Standard Quantum Limit (SQL) [2]. With this implementation, GQuEST will be dominated by classical noise.

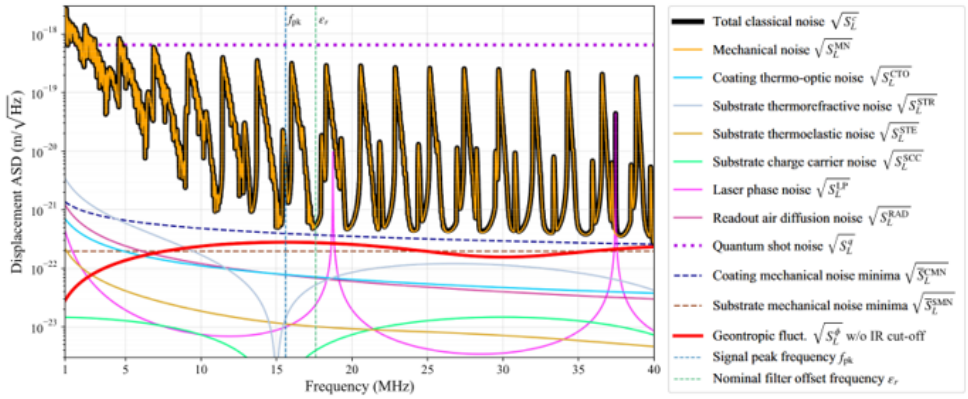


Figure 2: GQuEST noise by source [2].

In order to extract information from the photon-counting readout, GQuEST will also use a homodyne readout scheme to characterize the classical noise of the system to subtract from the data.

1.2 Cross-Correlation

Cross-correlation allows us to measure two signals and remove uncorrelated signals (e.g., quantum shot noise) while keeping correlated signals (e.g., amplitude fluctuations due to real spacetime fluctuations). GQuEST's homodyne detection system will use two photodetectors routed to two channels in the ADC, where the data is digitized, windowed, and Fast Fourier Transforms (FFTs) are performed. For a continuous function, the cross-correlation is found by

$$(f \star g)(\tau) = \int_{-\infty}^{\infty} (f^*(t)g(t+\tau))dt \tag{1}$$

where τ is the time lag or displacement between the two signals.

GQuEST's signal processing system will use the cross spectral density (CSD) to get frequency information. This is equivalent to the Fourier transform of the cross-correlation:

$$S_{FG}(f) = \mathcal{F}(f \star g)(\tau)(f) \tag{2}$$
$$= \int_{-\infty}^{\infty} \left(\int_{-\infty}^{\infty} f^*(t)\, g(t+\tau)\, dt \right) e^{-2i\pi f\tau}\, d\tau \tag{3}$$
$$= F^*(f)\, G(f) \tag{4}$$

We use $\tau = 0$ because we expect any real signal to be in phase between the two photodetectors. The real data consist of a discrete number of FFTs, and are integrated over a finite number of frames so the CSD is

$$S_{FG}(f) = \frac{1}{N} \sum_{i=1}^{N} (F_i^*(f) G_i(f)) \tag{5}$$

The data acquisition system allows us to choose the FFT window length Δt, and each FFT is saved as a "frame." The data is then accumulated and averaged into "superframes" with a certain overlap (usually 50% per Welch's method) between frames.

2 Objectives

The initial goals of this project were:

- To test a modified photodiode's frequency response and replicate the modifications on a second photodiode for use in cross-correlation measurements.
- To create data acquisition code based on the code from the Holometer experiment.
- To measure the ADC's cross-correlated noise floor.
- To measure the laser noise at 17 MHz.

3 Approach

3.1 Photodiode Modifications

My advisor modified a Thorlabs PDA05CF photodetector to be able to receive higher power by adding an inductor/resistor pair to lower the voltage gain (approximately 0.1 the initial

value) at DC, while retaining high gain at RF. I replicated these modifications to a second photodiode to use for cross-correlation measurements.

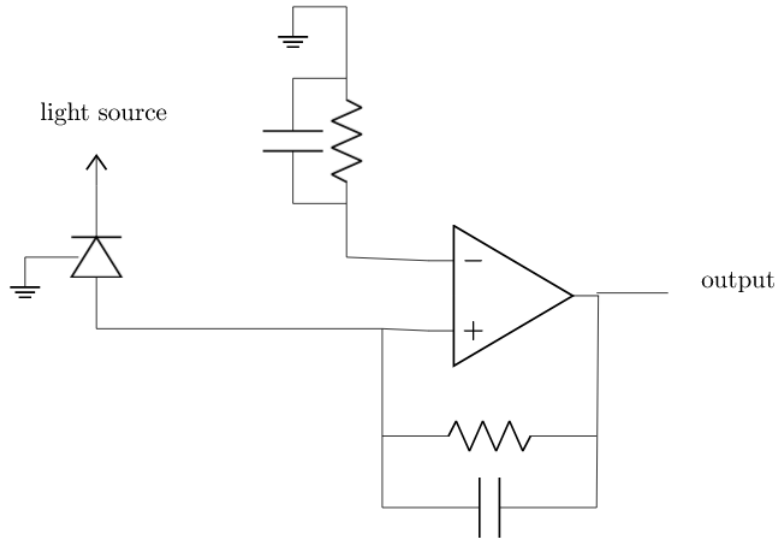


Figure 3: Unmodified Photodetector Circuit Schematic

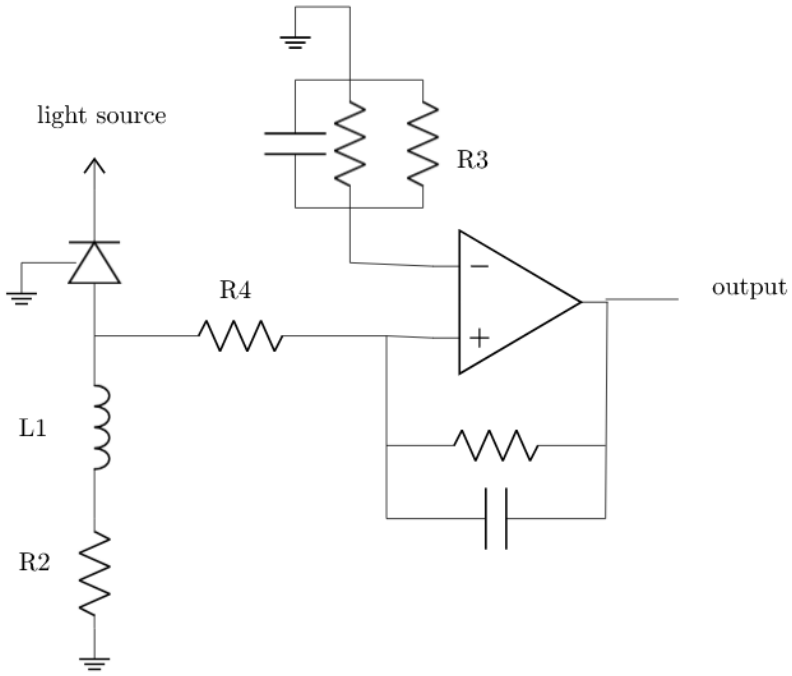


Figure 4: Modified Photodetector Circuit Schematic

I measured the actual inductance and resistance of the added components in both photode-

tectors:

Component	Expected value	Measured value (photodetector A)	Measured value (photodetector B)
L_1	10μH	10.5μH (0.6Ω)	10.7μH (0.8Ω)
R_2	4.7Ω	6.1Ω	6.4Ω
R_3	51Ω	49.7Ω	52.2Ω
R_4	51Ω	50.5Ω	53.8Ω

Table 1: Expected vs measured inductance and resistance of added components

Based on the alterations, we theoretically expect to see a decrease in voltage gain at DC. For the expected values, the ratio of the voltage gain of a modified detector at DC to the voltage gain of an unmodified detector at DC is:

$$\frac{V_{mod}}{V_{unmod}} = \frac{R_1 + R_2}{R_4} \tag{6}$$

$$= \frac{4.7}{51} \tag{7}$$

$$= 0.092 \tag{8}$$

For photodetector A, this ratio is actually

$$\frac{R_1 + R_2}{R_4} = \frac{6.1 + 0.6}{50.5} \tag{9}$$

$$= 0.133 \tag{10}$$

For photodetector B, this ratio is actually

$$\frac{R_1 + R_2}{R_4} = \frac{6.4 + 0.8}{53.8} \tag{11}$$

$$= 0.134 \tag{12}$$

3.2 Photodiode Characterization

I built a circuit to use to test the frequency response of the original modified photodiode and compare it to an unmodified model. We need to characterize these photodiodes for future use in quantifying laser and mechanical noise in the interferometer and filter cavities for fine tuning the GQuEST experiment.

I used a bias tee circuit to power an LED. I built the circuit on a breadboard, powered with 6-8 V DC, and initially tested the circuit outputs on various inputs using a Siglent oscilloscope and a Moku Go. The photodiode showed a peak at the modulation frequency with 400 mVpp - 1 Vpp. I attempted to use a 1550 nm (Thorlabs LED1550L), 780 nm (Thorlabs LED780L), and 570 nm LED on the photodiode to get the frequency response function, but switched to a 685 nm laser diode (Thorlabs HL6750MG) for a stronger output signal.

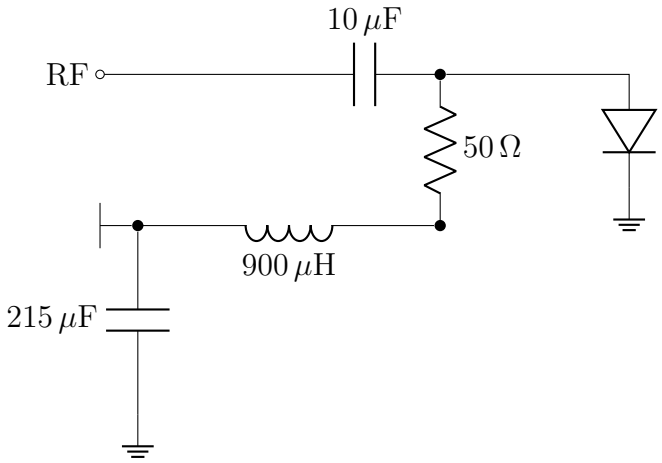


Figure 5: Bias tee circuit used to modulate 685 nm laser diode

The photodiode used is an indium gallium arsenide (InGaAs) fixed-gain amplified detector. The frequency response was tested using the same circuit powered with 8 V DC (with 100 mA current limit) and swept from 1 kHz to 10 MHz with 1 Vpp AC.

The frequency response function of the modified photodiode and an unmodified photodiode confirmed the expected results. At DC, the modified photodiode is theoretically expected to have around 0.1 the amplitude of the unmodified one, while they perform similarly at high frequencies.

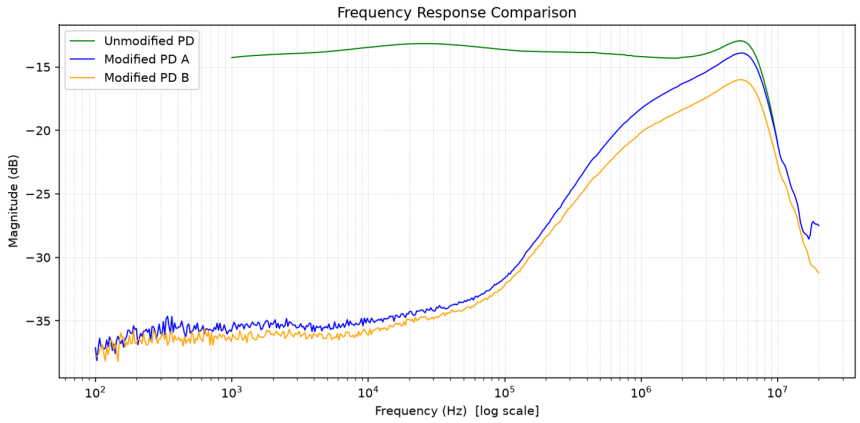


Figure 6: Frequency response of modified and unmodified photodetectors

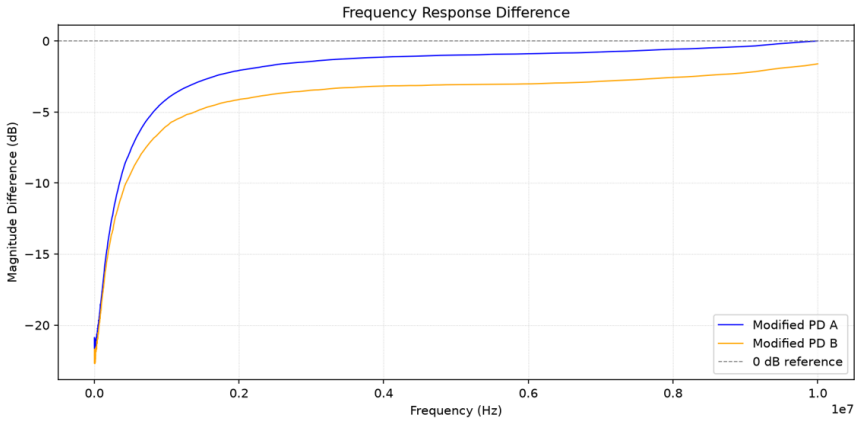


Figure 7: Difference in frequency response of modified and unmodified photodetectors

Figures 6 and 7 clearly show that the modified photodiode has ∼20 dB lower amplitude (10%) than the unmodified at DC, but the two remain within 1 dB at high frequency.

Furthermore, I compared modified photodetector A with modified photodetector B, which revealed that photodetector B had lower voltage gain across all frequencies. However, the two were mostly within 2 dB, which is a reasonable difference which we can account for during cross-correlation.

3.3 Data Acquisition System

GQuEST's data acquisition code is modeled after that of the Holometer experiment [3]. I modified the existing C++ and Python code from the Holometer experiment to interface with GQuEST's 4-channel, 16-Bit, 125 MS/s per channel PCIE-1840 digitizer from Advantech.

The photodetector measures the incident power of the light as a voltage, and the digitizer discretizes the data by sampling at a given frequency (80 MHz). The program then windows the data to perform Fourier transforms. The software allows the user to select any power of 2 as the number of data points used in each FFT, with the default being $N = 2^{16} = 65536$, as used for the Holometer [3]. Each FFT constitutes one frame, and each frame has a 50% overlap with its neighboring frames (each data point is used in two distinct FFT frames). Assuming the signal is stationary, we process the data using these frames and then average over a number of frames to get the final results.

Given that GQuEST is looking for signals on the order of MHz, it needs to have a MHz sampling rate. 80 MHz was chosen to allow sensitivity up to 20 MHz, slightly above the signal frequency of 17 MHz. This results in an enormous rate of data acquisition which is unfeasible to store. As a result, we will store only time-averaged spectra, which are calculated in real time.

After obtaining the N frames, we apply a Fourier transform. First, we apply the Hann

window function to attenuate the ends of the frame in order to reduce spectral leakage[4]:

$$w_n = \frac{1}{2}[1 - \cos(\frac{2\pi n}{N})] \tag{13}$$

Next, we perform a Fast Fourier Transform on the data and average over all frames. We can then store the resulting averaged vectors in a covariance matrix, where the diagonal elements represent the time-averaged power spectrum of each channel and the off-diagonal elements represent the time-averaged cross-correlations between channels [3]. The matrix is symmetric so we can set the lower triangular elements to 0.

Each matrix contains 4 real diagonal elements, each 64 bits or 8 bytes. The 6 complex off-diagonal elements are represented by 2 floating point numbers, so require 16 bytes. This means each matrix requires 128 bytes of storage.

The frequency bin count is a function of the number of samples per frame, as it requires more points to resolve greater frequency resolution. This is given by

$$\#\text{ frequency bins} \approx \frac{N}{2} = \frac{2^{16}}{2} = 32,768 \tag{14}$$

So the software saves 32,768 128-byte covariance matrices for each frame; therefore the amount of data for each frame is:

$$128\text{ bytes} \times 32,768\text{ per frame} = 4,194,304\text{ bytes/frame} \approx 4.19\text{ MB/frame} \tag{15}$$

This is a significant amount of data, and with 2^{16} samples/frame at a 80 MHz sampling rate with a 50 % frame Welch overlap, this corresponds to 2441.4 frames per second, or 10.24 GB/s. It would be impossible to save all of this data, so we instead save a sum of many frames over a 5 second "superframe". This reduces the data rate to 839 kB/s, which is much more reasonable. We assume that the power spectrum is linear and time-invariant to a good approximation, so we do not lose information by performing this compression.

The raw data rate per channel is 160 MB/s, since the sampling rate is 80 MHz and each voltage value is saved as a 16-bit integer (2 bytes). Since the ADC has 4 channels, this is 640 MB/s

$$\frac{640\text{ MB/s}}{839\text{ kB/s}} = 762.8 \tag{16}$$

This process offers roughly 763-fold compression, and will reduce the total data footprint substantially, allowing for long-term integration without exceeding storage limits. In order

to process the data as fast as it is collected, the program must perform FFTs as fast as each frame takes, which is equal to the integration time of ∼0.8 ms. Therefore, the program must be optimized, and the limits of the hardware and the program speed (specifically, FFT calculation) must be taken into account when determining the integration time.

To create this software, we created an interface between the Advantech ADC data acquisition code and the Holometer data acquisition and signal processing code. The following provides a brief sketch of the data flow in each system and how the interface works.

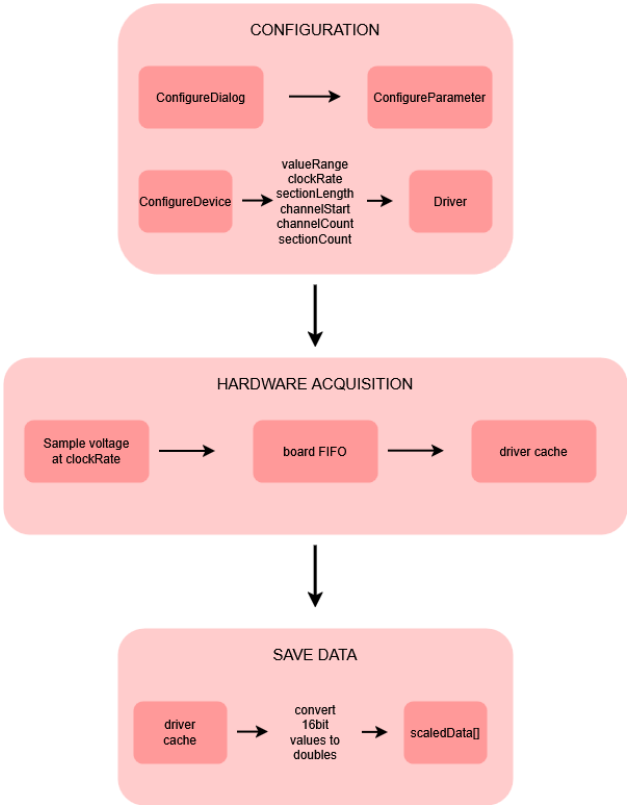


Figure 8: Advantech ADC data acquisition

Essentially, the Advantech code provides a prebuilt system for analog input data acquisition. This allows the user to edit the number of channels and the sampling rate used, which is then sent to the hardware. The voltages are sampled at the chosen clock rate and stored as 16-bit integers on the board, and then send to the computer where it is then converted into doubles and stored in an array. For our purposes, we will actually leave the voltages as 16-bit integers, as the signal processing code takes 16-bit integers as input.

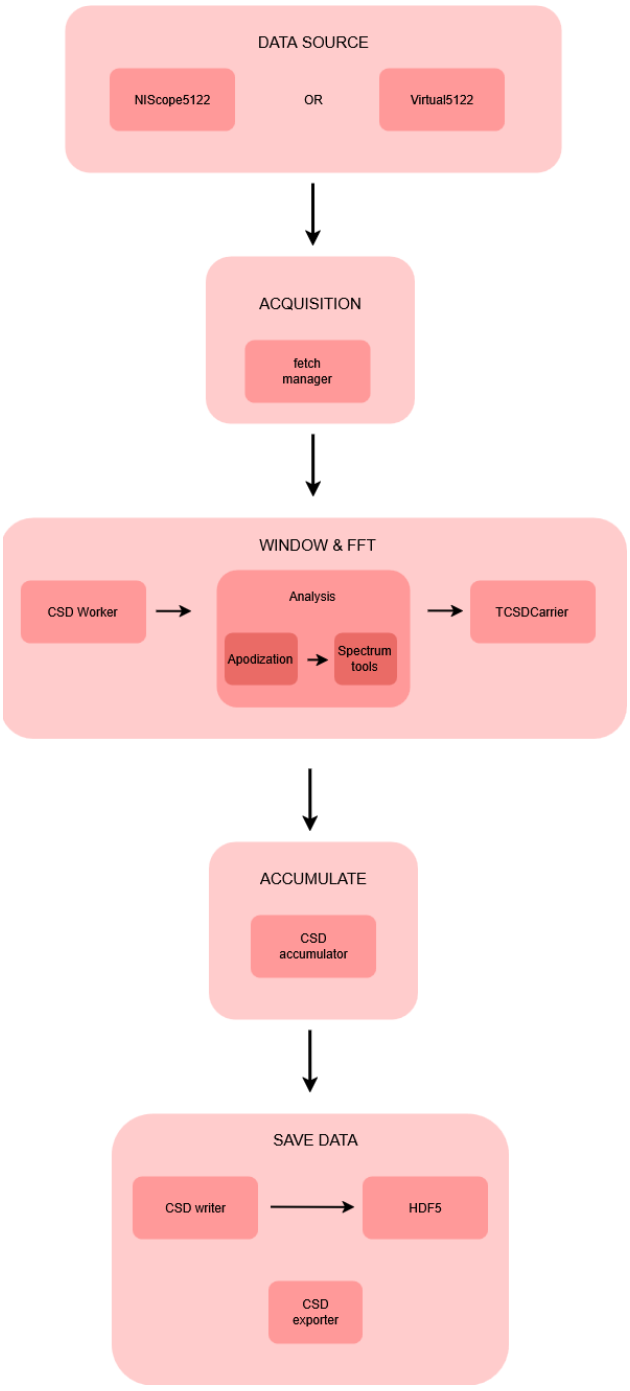


Figure 9: Fermilab Holometer data acquisition and signal processing

The signal processing code takes voltage values (either from a real ADC or simulated source), where it is windowed (apodization) and FFTs are performed (spectrum tools). Then, it is accumulated and saved.

We built a new data source into the Holometer data acquisition code for GQuEST's Advantech ADC. This mimicked the NIScope5122 data source while also implementing all of the necessary hardware configuration from Advantech's existing analog-in code.

Furthermore, we added additional files to the system to adjust configurable settings such as AC/DC coupling, impedance, voltage range, and runtime.

3.4 Theoretical ADC Noise Floor and Required Runtime

We need to know the cross-correlated electronic noise floor of the ADC before using it for any real measurements. I first calculated the theoretical noise floor to determine how long we needed to run the system to resolve the noise floor.

The correlated noise decreases with time, eventually reaching a real correlated noise floor:

$$\langle S_{CSD} \rangle_{t \to \infty} = S_q^{\text{corr}} \tag{17}$$

$$\langle S_{CSD} \rangle(t) = \frac{\sqrt{S_0 S_1}}{N_{\text{avg}}(t)} + S_q^{\text{corr}} \tag{18}$$

The fundamental noise dominating each individual channel is quantization noise, given by:

$$\sigma_q = \frac{V_{\text{pp}}}{\sqrt{12} \times 2^{N_{\text{bits}}}} \tag{19}$$

For the Advantech ADC hardware, $N_{\text{bits}} = 16$. Thus the theoretical noise floor given this quantization noise is:

$$\sigma_q^2 = \int_0^{\Delta f} S_q(f) df \tag{20}$$

$$= \int_{0\ \text{Hz}}^{40\,\text{MHz}} S_q(f) df \tag{21}$$

$$= S_q \times 40\,\text{MHz} \tag{22}$$

The cross-correlated noise must be less than the individual channel noise, so for some factor $\gamma \in (0, 1)$, the cross-correlated noise is:

$$S_q^{\text{corr}} = \gamma \sqrt{S_{q0} S_{q1}} \tag{23}$$

$$= \gamma S_q \tag{24}$$

Given the parameters of the hardware used and the standard deviation of the injected noise σ_V, the theoretical noise floor of each channel is:

$$S_q = \frac{\sigma_q^2}{40\,\mathrm{MHz}} \tag{25}$$
$$= \frac{(\frac{V_{\mathrm{pp}}}{\sqrt{12}\times 2^{N_{\mathrm{bits}}}})^2}{40\,\mathrm{MHz}} \tag{26}$$
$$= \frac{V_{\mathrm{pp}}^2}{12\times 2^{32}\times 40\times 10^6\ \mathrm{Hz}} \tag{27}$$

GQuEST will likely use the ADC with a voltage range of $-1\,\mathrm{V}$ to $1\,\mathrm{V}$, therefore the individual channel ADC noise floor is estimated:

$$S_q = \frac{(2\,\mathrm{V})^2}{12\times 2^{32}\times 40\times 10^6\ \mathrm{Hz}} \tag{28}$$
$$= 1.940\times 10^{-18}\ \mathrm{V}^2/\mathrm{Hz} \tag{29}$$

Depending on the factor γ, the correlated value could be much smaller. To properly resolve this, we would like $\frac{\sqrt{S_0 S_1}}{N_{avg}}$ to be an order of magnitude less than S_q. The waveform generators we are using have a minimum possible σ_V of $0.1\,\mathrm{mV}$, but we can use 10 mV on each channel:

$$\sqrt{S_0 S_1} = S \tag{30}$$
$$\sqrt{S_0 S_1} = \sqrt{\frac{\sigma_{V0}^2}{20\,\mathrm{MHz}}\cdot\frac{\sigma_{V1}^2}{20\,\mathrm{MHz}}} \tag{31}$$
$$= \frac{\sigma_{V0}\sigma_{V1}}{20\,\mathrm{MHz}} \tag{32}$$
$$= \frac{(10\times 10^{-3}V)(10\times 10^{-3})}{20\,\mathrm{MHz}} \tag{33}$$
$$= 5\times 10^{-12}\ \mathrm{V}^2/\mathrm{Hz} \tag{34}$$

So to get $N_{\mathrm{avg}} \geq (10)\frac{S}{S_q^{\mathrm{corr}}}$:

$$N_{\mathrm{avg}} \geq (10)\frac{S}{S_q^{\mathrm{corr}}} \tag{35}$$
$$\geq (10)\frac{5\times 10^{-12}\ \mathrm{V}^2/\mathrm{Hz}}{1.940\times 10^{-18}\ \mathrm{V}^2/\mathrm{Hz}} \tag{36}$$
$$\geq 2.58\times 10^7 \tag{37}$$

Therefore, we will aim for 3×10^7 frames. We can set the number of points in each frame to any power of 2, so by choosing 2^{11} we find the frames per second n (given that the 50% overlap means we collect twice as many frames):

$$n = 2 \times \frac{80 \times 10^6}{2^{11}} \text{ frames/s} \tag{38}$$

$$= 78125 \text{ frames/s} \tag{39}$$

Therefore, we must run the ADC and collect frames for 384 seconds, or around 6.4 minutes. Then, we must average all 3×10^7 frames to resolve the true correlated noise floor. We tried this type of measurement in several configurations, but actually were able to get the best data from running on 50Ω terminated channels (which should hit the noise floor before the injected noise measurement). Therefore, by running for 30 minutes, we are reasonably confident we have resolved the noise floor even if the correlated noise is much smaller than the individual channel quantization noise, say $\gamma = 0.05$.

3.5 17 MHz Laser Noise Measurement

Cross-correlating two interferometers theoretically eliminates all uncorrelated quantum and classical noise sources. However, both single photon counting and cross-correlated homodyne readout should be able to eliminate quantum shot noise even with a single interferometer, so the initial signals we will be reading will be dominated by classical noise sources such as laser noise. Since GQuEST is searching for signals at 17 MHz, we characterized the laser noise at this frequency.

We built a fiber optic Mach-Zehnder interferometer. One arm of the interferometer has a path length 5 m greater than the other. As a result, we will measure any frequency noise in the laser at 17 MHz as a phase difference in the two photodetectors.

It takes light 24.2 ns to travel 5 m in an optical fiber:

$$\tau = \frac{n \cdot \Delta L}{c} \tag{40}$$

$$= \frac{1.45 \cdot 5\text{m}}{3 \times 10^8 \text{m/s}} \tag{41}$$

$$= 24.2 \text{ ns} \tag{42}$$

The interferometer has maximum sensitivity when the delay between the signals is half of the signal period, the period of the signal shoudl be 2x the arm travel time. The period of a 17 MHz sine wave is 58.8 ns ($T = \frac{1}{f} = \frac{1}{17 \times 10^6}$). This is roughly 2 times the travel time of the interferometer arm difference, so it can resolve 17 MHz noise well.

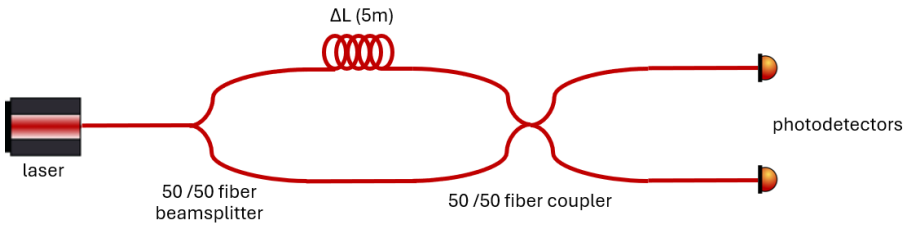


Figure 10: IFO for laser noise measurement schematic

4 Results

Using the technique of cross-correlation as described above, we were able to produce an estimate of the noise floors of several hardware systems for GQuEST. We estimate the electronics noise of the ADC itself to be around $10^{-9}\mathrm{V}/\sqrt{\mathrm{Hz}}$ with some higher peaks across the frequency spectrum. This estimate was produced by running the data acquisition code for around 30.5 minutes on 2 channels of the ADC, each of which was 50 Ω terminated.

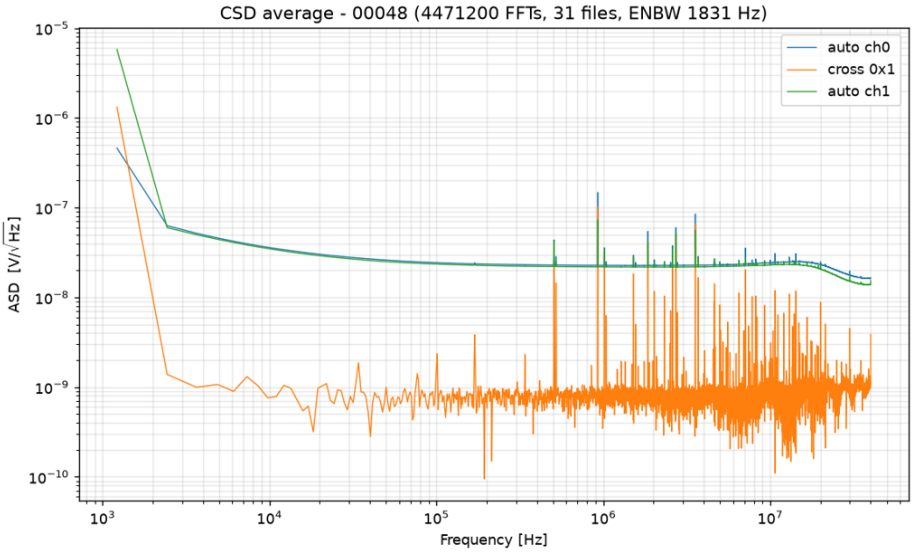


Figure 11: ADC cross-correlated noise floor

This is close to the estimated value of $< 1.39 \times 10^{-9}\mathrm{V}/\sqrt{\mathrm{Hz}}$, based on the above estimate of 1.940×10^{-18} V^2/Hz quantization noise in each channel. In addition to the calculations estimating the necessary runtime, we also graphed the band median over time, excluding the first and last frequency bins. This shows that the CSD values leveled out to a constant value, indicating that the measurement reached the true noise floor of the system.

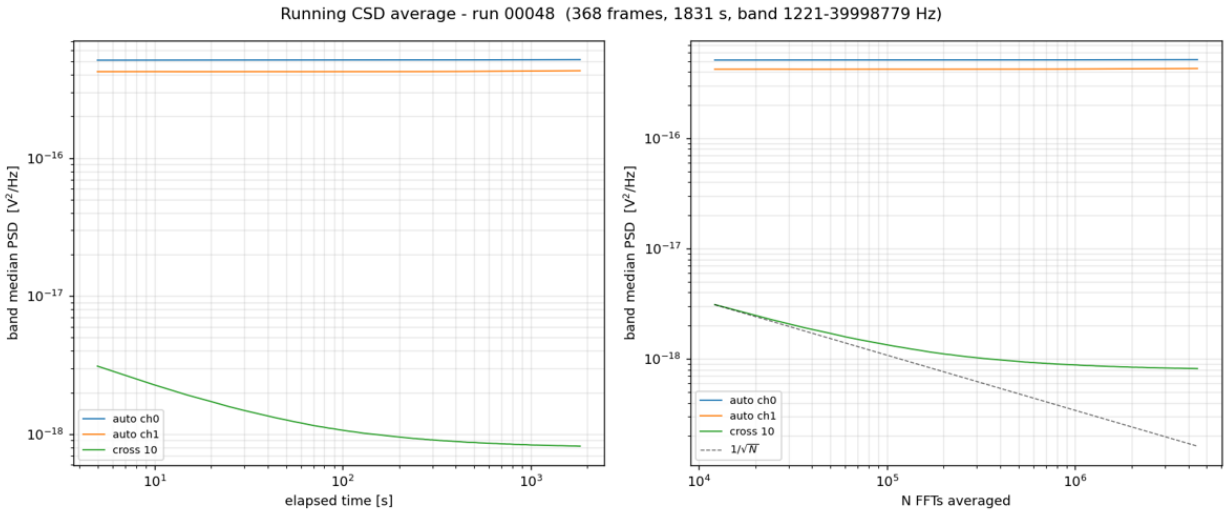


Figure 12: ADC CSD band median over time

We also measured the electronics noise of the unmodified Thorlabs photodetectors by cross-correlating dark current signals from two photodetectors with caps over the diodes. We ran this measurement for around 61 minutes. Using the quantum efficiency of the photodiodes and the transimpedance gain of the circuit, we find the cross spectral density in $\mathrm{W}/\sqrt{\mathrm{Hz}}$:

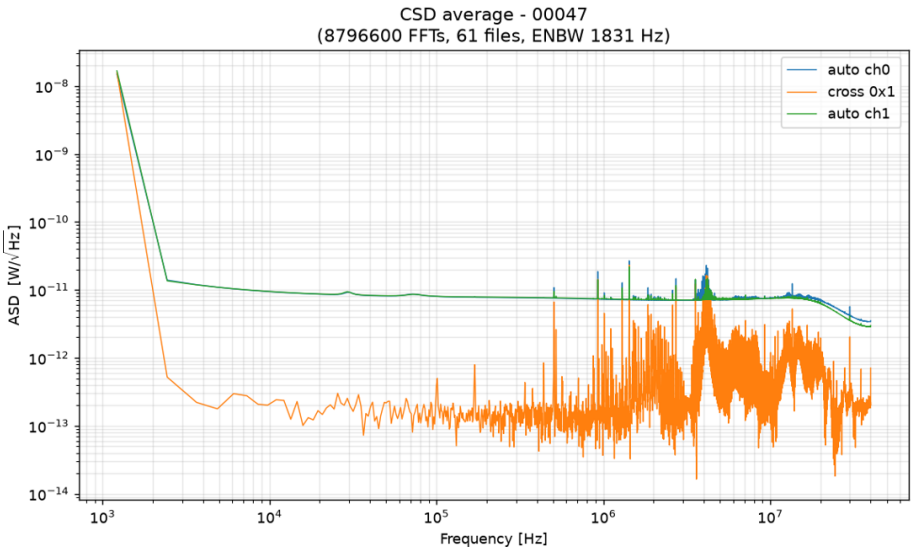


Figure 13: Unmodified PDs cross-correlated noise floor

Since the modified photodetectors' transfer function varies significantly with frequency, we used the difference in magnitude of the transfer functions of the modified and unmodified photodetectors to calibrate the data, in addition to the quantum efficiency and transimpedance gain information. We ran this measurement for around 13.48 hours. This resulted in the following cross spectral density in $\mathrm{W}/\sqrt{\mathrm{Hz}}$ for the modified photodetectors:

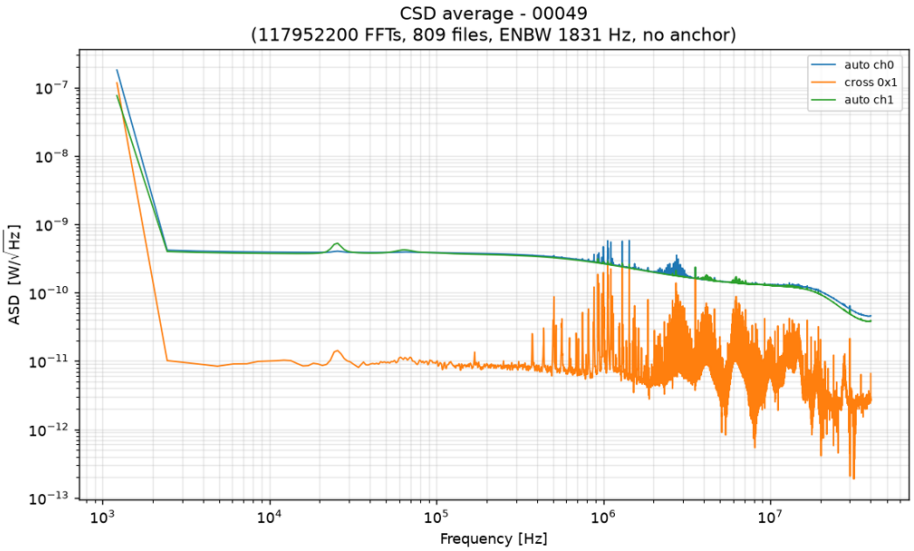


Figure 14: Modified PDs cross-correlated noise floor

We also have some preliminary data showing the cross-correlated outputs from the Mach-Zehnder interferometer.

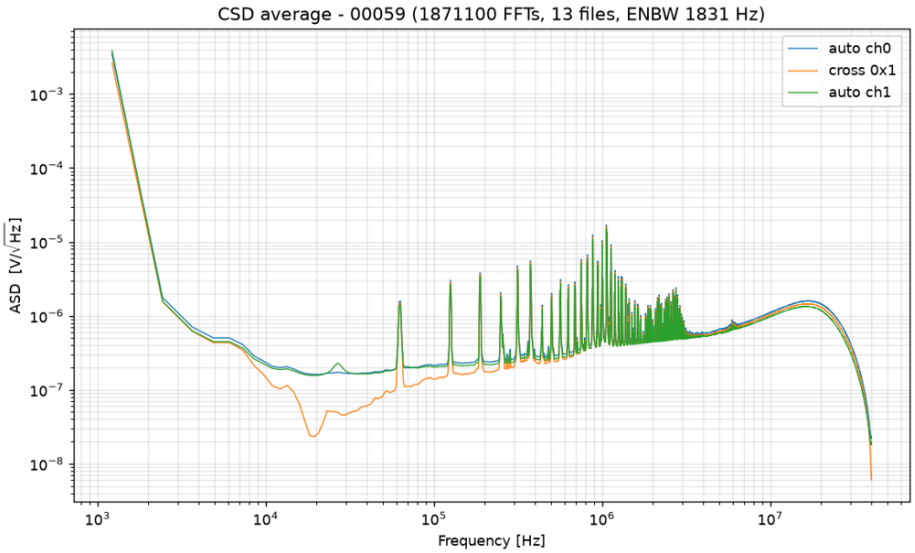


Figure 15: ASD from Mach-Zehnder IFO

5 Conclusion

In order to effectively characterize all of the classical noise present in the GQuEST experiment, we will need to obtain final estimates of the 17 MHz laser phase noise and the laser

relative intensity noise, and once the GQuEST interferometer is assembled we will quantify other sources of classical noise such as the noise from the mirrors.

This work provides helpful estimates of several of the classical noise sources in GQuEST, which will be necessary for extracting the signal from the photon-counting readout. For instance, the ADC electronics noise floor sits below the noise of the photodetectors across most of the spectrum, and will likely not be a dominant noise source in data from the homodyne readout.

6 Acknowledgements

Thank you to my advisor Lee McCuller and my mentors Sander Vermeulen and Alexander Ramirez for all of their support with this project. This work was made possible by funding from the National Science Foundation, LIGO Laboratory, and the California Institute of Technology.

References

[1]E. Verlinde and K. M. Zurek, "Modular fluctuations from shockwave geometries", Phys. Rev. D **106**, 106011 (2022).

[2]S. M. Vermeulen, T. Cullen, D. Grass, I. A. O. MacMillan, A. J. Ramirez, J. Wack, B. Korzh, V. S. H. Lee, K. M. Zurek, C. Stoughton, and L. McCuller, "Photon-counting interferometry to detect geontropic space-time fluctuations with GQUEST", Physical Review X **15**, 011034 (2025).

[3]J. Richardson, *The Holometer data acquisition system*, Technical Document, Details the data processing computation performed by the Julie Stream data acquisition code (Fermi National Accelerator Laboratory, June 2013).

[4]M. Cerna and A. F. Harvey, *The fundamentals of FFT-based signal analysis and measurement*, Application Note 041 (National Instruments, July 2000).